

# Supporting Information

## Construction of a Unique Two-Dimensional Hierarchical Carbon

### Architecture for Superior Lithium Ion Storage

Zhijie Wang,<sup>1</sup> Xiaoliang Yu,<sup>2</sup> Wenhui He,<sup>3</sup> Yusuf Valentino Kaneti,<sup>2</sup> Da Han,<sup>2</sup> Qi Sun,<sup>1</sup> Yan-Bing He,<sup>2\*</sup> Bin Xiang<sup>1\*</sup>

<sup>1</sup>Department of Materials Science & Engineering, CAS Key Lab of Materials for Energy Conversion, Synergetic Innovation Center of Quantum Information Quantum Physics, University of Science and Technology of China, Hefei, Anhui 230026, China

<sup>2</sup>Engineering Laboratory for the Next Generation Power and Energy Storage Batteries, and Engineering Laboratory for Functionalized Carbon Materials, Graduate School at Shenzhen, Tsinghua University, Shenzhen 100084, China

<sup>3</sup>Laboratory of Physics and Chemistry of Nano-Objects (LPCNO), Institut National des Sciences Appliquées de Toulouse (INSA), Paul Sabatier University - Toulouse III, Toulouse 31062, France.

\*Corresponding author: [binxiang@ustc.edu.cn](mailto:binxiang@ustc.edu.cn) (Bin Xiang); [he.yanbing@sz.tsinghua.edu.cn](mailto:he.yanbing@sz.tsinghua.edu.cn) (Yan-Bing He).

## Methods

**Preparation of Mg-Al LDH and Mg-Al LDO** Mg-Al LDH was synthesized via a co-precipitation method.  $\text{Mg}(\text{NO}_3)_2 \cdot 6\text{H}_2\text{O}$  (12.82 g),  $\text{Al}(\text{NO}_3)_3 \cdot 9\text{H}_2\text{O}$  (9.38g) (Mg/Al molar ratio is 2), and urea (90.09 g) were dissolved in 500 ml of deionized (DI) water and transferred into a round-bottom flask. Under reflux condensation, the solution was maintained at 100 °C for 12 h under magnetic stirring. Following this, the temperature was decreased to 94 °C and maintained for another 12 h without stirring. After vacuum filtration, washing with DI water and freeze drying, Mg-Al LDH was obtained. Finally, the as prepared Mg-Al LDH was calcined at 500 °C for 3 h in air and then ground in an agate mortar to obtain Mg-Al LDO.

**Dye adsorption** 150 ml of DI water was filled into a 250 ml three-mouth-flask. After purging with argon for 30 min to drive carbon dioxide out, 0.6 g of Orange II was dispersed into the DI water. Then, 1 g of Mg-Al LDO was added into the solution to adsorb the dye for 48 hours. Magnetic stirring and argon protection were maintained during the whole adsorption process. Afterwards, the solution was vacuum filtrated and washed with DI water, then the obtained powder (RLDH/OII) was freeze dried and ground. In order to investigate the formation mechanism of RLDH/OII 2D hierarchical structure, a reference experiment was conducted. LDO was put into pure deionized water and stirred continuously for 48 h.

**Carbonization of RLDH/OII** The carbonization of RLDH/OII was conducted in a horizontal tube furnace at 800 °C for 2 h under argon atmosphere with a heating rate of 2 °C/min. Then the obtained black powder was washed with HCl (6M) and NaOH (2M) respectively at 70 °C for 6 h. After freeze drying, the target product 2D-HCA was obtained. For comparison, Orange II was directly carbonized and washed with the same conditions to get the reference sample C-OII.

**Microstructure Characterization** The morphologies and structures of the samples were

examined by a field emission scanning electron microscopy (FESEM, ZEISS SUPRA 55) and a field high resolution transmission electron microscopy (HRTEM, JEM-2100F). The powder X-ray diffraction (XRD) patterns were measured using a Rigaku D/max 2500/PC diffractometer (Cu-K $\alpha$  radiation with  $\lambda = 1.5418 \text{ \AA}$ ). A laser with excitation wavelength of 532 nm on a HORIBA Labram HR Evolution Raman spectrometer was used to measure the Raman spectra of the samples (at room temperature). The nitrogen adsorption/desorption isotherm was measured at 77 K using an automated adsorption apparatus (Micromeritics ASAP 2020). Brunauer-Emmett-Teller (BET) equation was used to determine the specific surface area, and density functional theory (DFT) was utilized to calculate the pore size distribution. An ESCALAB 250X spectrometer was used for X-ray photoelectron spectroscopy (XPS) analysis.

**Electrochemical Tests** The lithium storage properties of 2D-HCA and C-OII were tested at room temperature using coin-type cells (CR2032). A slurry consisted 70 wt % of 2D-HCA (or C-OII), 20 wt % of poly (vinylidene fluoride) and 10 wt % of acetylene black in N-methyl pyrrolidone was coated on a copper foil. After being dried at 55 °C for 2 h and at 110°C for another 10 hours, the electrode was punched into disks with a diameter of 12 mm. 1.0 M LiPF<sub>6</sub> in 1:1 v/v ethylene carbonate/diethyl carbonate (EC/DEC) was used as the electrolyte. Lithium foil was used as both the counter electrode and reference electrode. Battery assembly was carried out in an argon-filled glove box with concentrations of moisture and oxygen below 1 ppm. Cyclic voltammetry was performed using an electrochemical workstation (CHI 660E) at a scanning rate of 0.2 mV s<sup>-1</sup> in the potential window of 0.005 V-3 V vs. Li/Li<sup>+</sup>. The cycling performance and rate capability were tested at certain current densities in the potential window of 0.005 V-3 V vs. Li/Li<sup>+</sup> using a LAND battery tester (CT2001A).

**Preparation for cycled electrodes analyses** The cycled batteries were opened in argon-filled glove box. After that, the electrodes were washed with electrolyte and dimethyl carbonate (DMC), and then dried in the glove box.

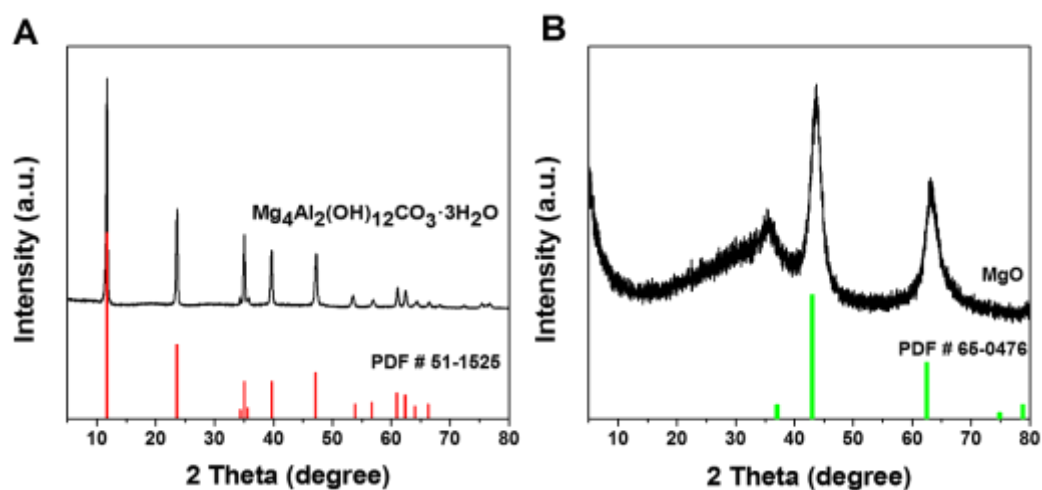


**Figure. S1.** XRD patterns of (A) LDH and (B) LDO. The diffraction peaks of LDH can be assigned to  $\text{Mg}_4\text{Al}_2(\text{OH})_{12}\text{CO}_3 \cdot 3\text{H}_2\text{O}$  ( $\text{Mg}_2\text{Al-LDH}$ ) (PDF # 51-1525). The Mg/Al ratio is 2 in our LDH. Interestingly, the diffraction peaks of LDO only can be assigned to MgO (PDF # 65-0476) and no diffraction peaks of  $\text{Al}_2\text{O}_3$  can be found. It is possible that the  $\text{Al}_2\text{O}_3$  phase in LDO is amorphous.

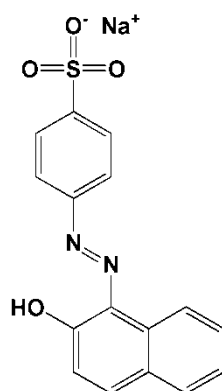


**Figure. S2.** Chemical structure of the organic anionic dye---Orange II (OII). The chemical formula of OII is  $\text{C}_{16}\text{H}_{11}\text{N}_2\text{O}_4\text{SNa}$ . The negatively charged organic group of  $\text{C}_{16}\text{H}_{11}\text{N}_2\text{O}_4\text{S}^{-1}$  can be absorbed as counter ions during Mg-Al LDO reconstruction process.

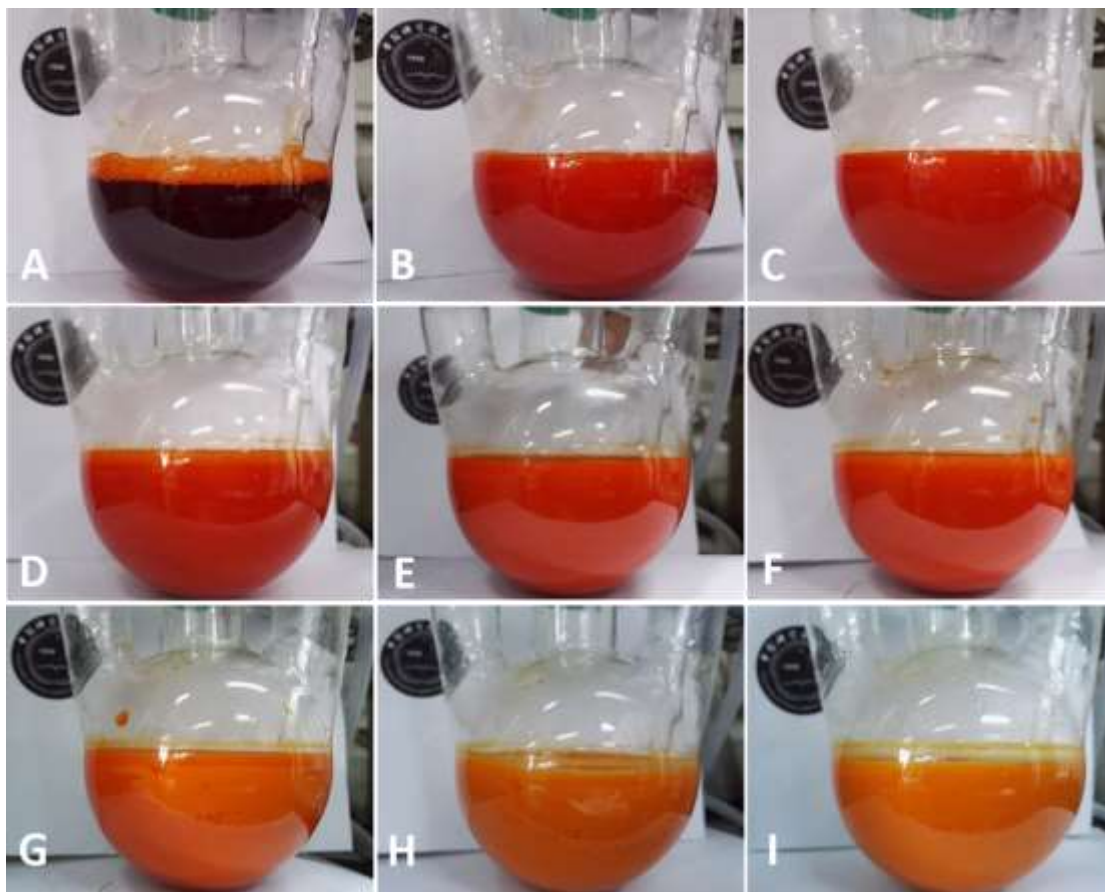


**Figure. S3.** Digital images of the solution during the adsorption process. (A) Pristine OII solution; (B) After LDO was added for 5 min and (C) 0.5h, (D) 1 h, (E) 3 h, (F) 6 h, (G) 19 h; (H) 24 h, (I) 48 h. The color of the solution gradually changes from red to orange, suggesting the successful adsorption of OII.

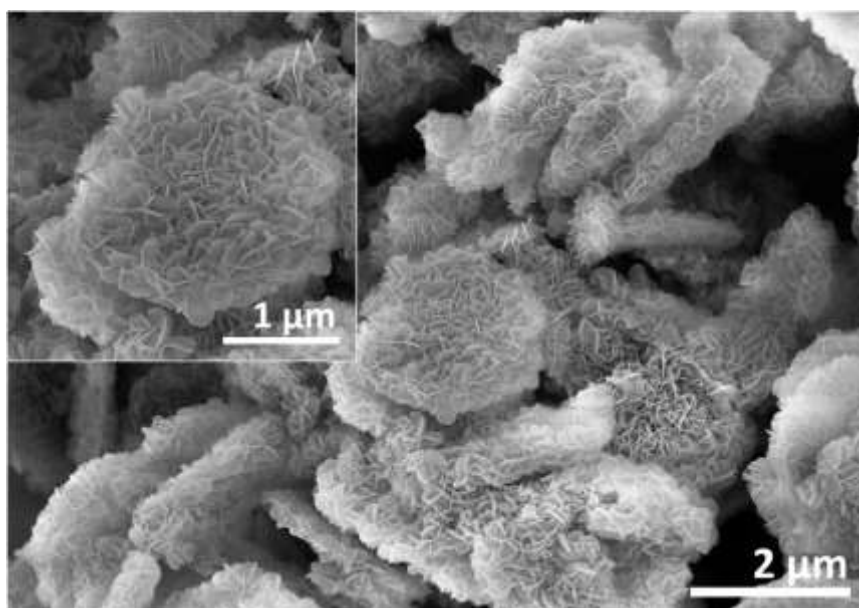


**Figure. S4.** SEM image of rehydrated LDH (RLDH). After being added into water and stirred for 48 h, LDO is reconstructed to RLDH by rehydration. The reconstructed LDH exhibits a

hierarchical structure composed of many nanosheets grown on the surface of hexagonal nanoplates.

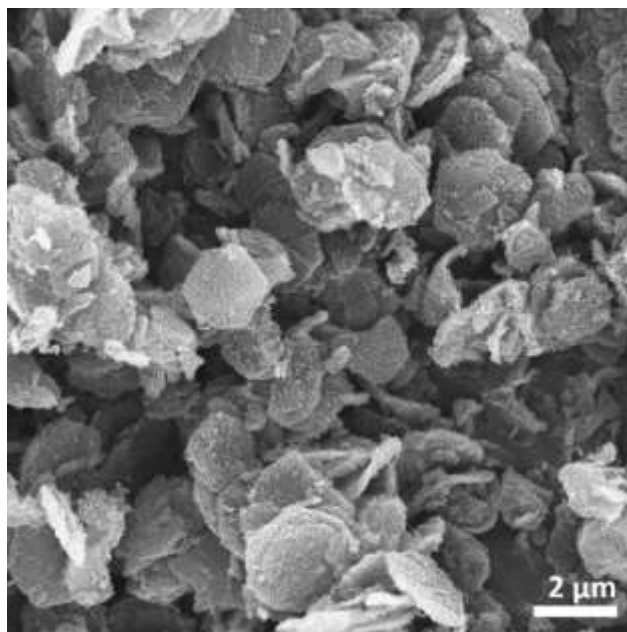


**Figure. S5.** Low magnification SEM image of 2D-HCA. No obvious aggregation can be observed.

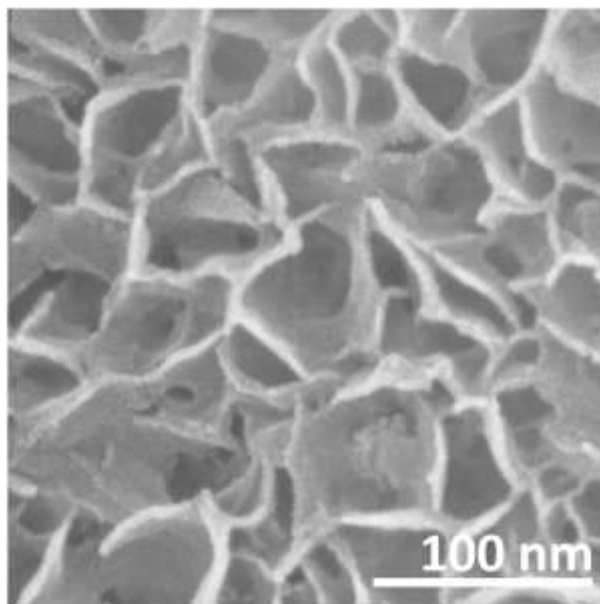


**Figure. S6.** High magnification SEM image of 2D-HCA.

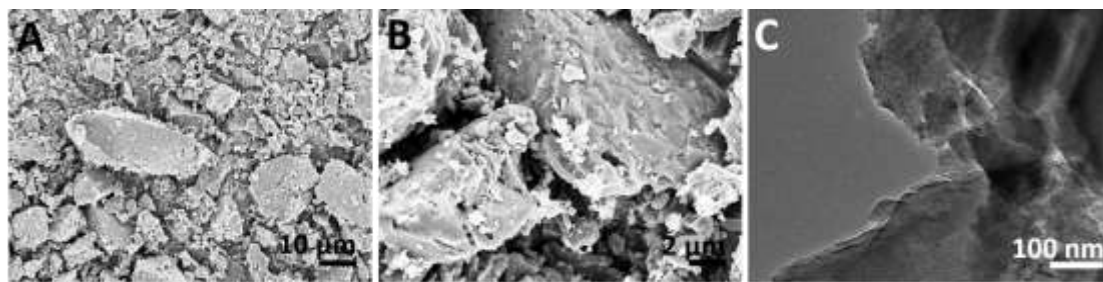


**Figure. S7.** (A) and (B) SEM images of C-OII at different magnifications; (C) TEM image of C-OII. The morphology of the C-OII is irregular blocky structure with sizes ranging from hundreds of nanometers to few tens of micrometers.

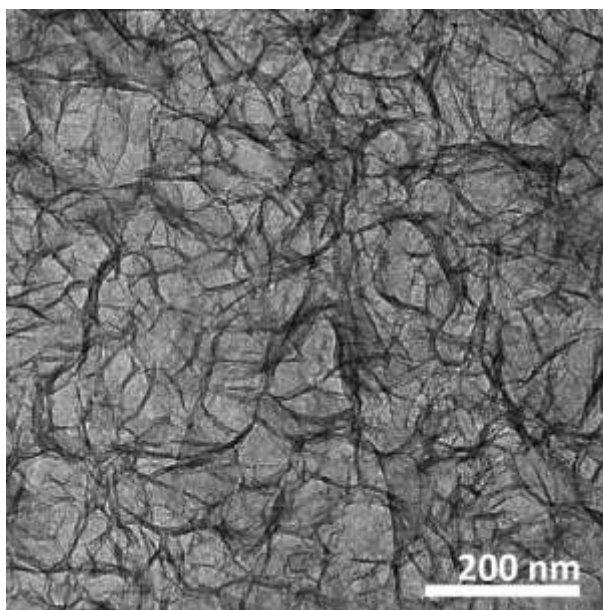


**Figure. S8.** High magnification TEM image of 2D-HCA, showing the interconnected macropores.

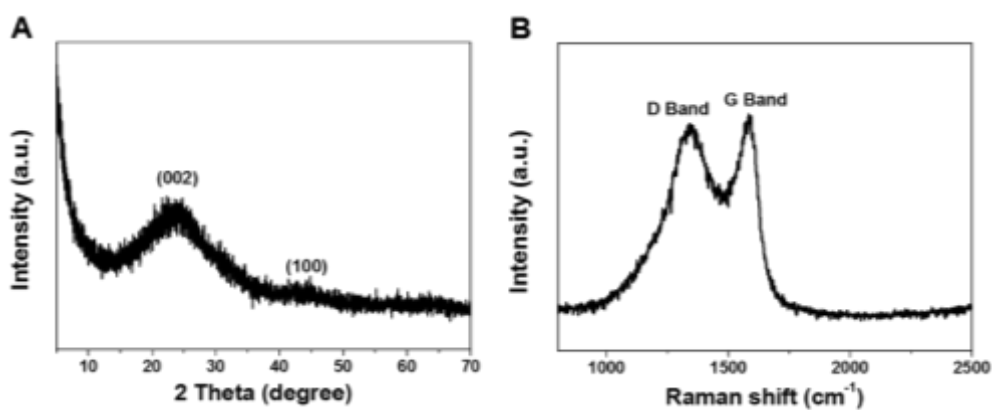


**Figure. S9.** (A) XRD pattern of 2D-HCA; (B) Raman spectrum of 2D-HCA.

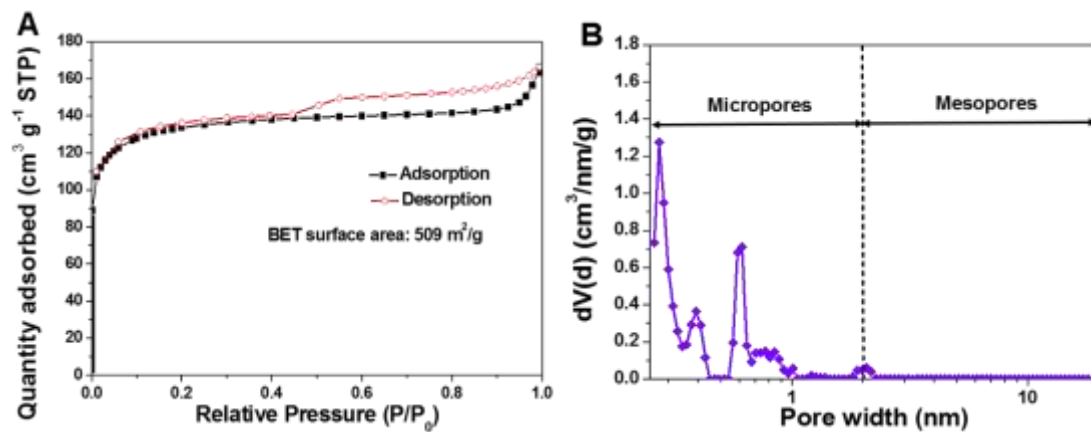


**Figure. S10.** (A) N<sub>2</sub> adsorption/desorption isotherms and (B) pore size distribution curves of C-OII.

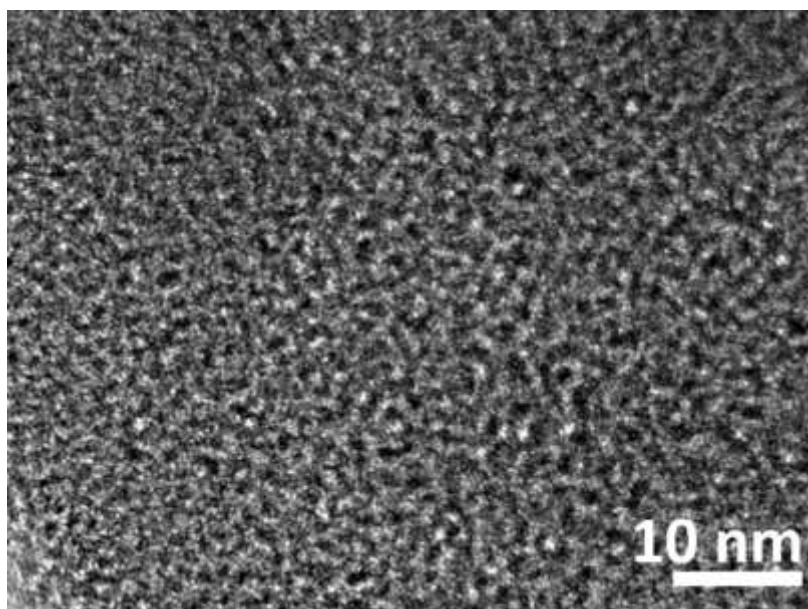


**Figure. S11.** HRTEM image of C-OII, which further verified the porous structure of C-OII, and plenty of small size pores can be observed in C-OII.



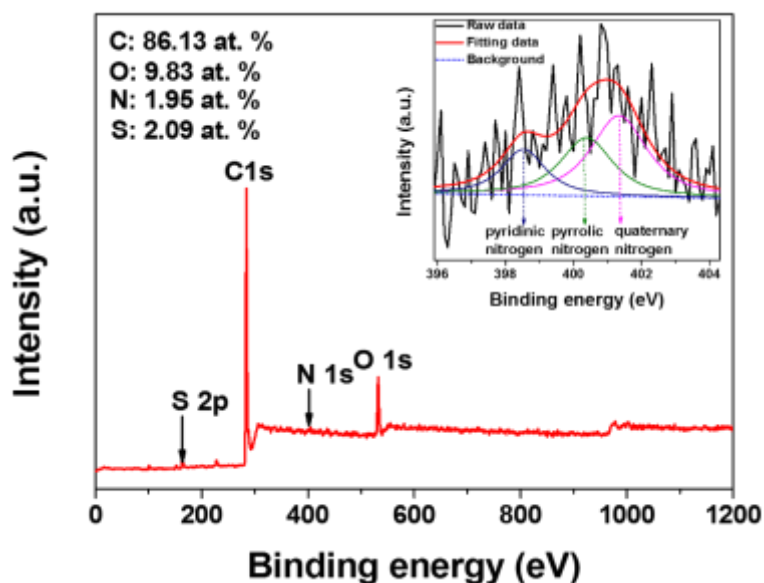


**Figure. S12.** XPS survey spectrum of 2D-HCA and high resolution XPS spectrum of N 1s (inset). C 1s, O 1s, N 1s, and S 2p peaks can be clearly observed from the XPS survey spectrum of the 2D-HCA; the corresponding concentrations of these elements are 86.13 at. %, 9.83 at. %, 1.95 at. % and 2.05 at. %, respectively. The spectrum of N 1s can be fitted into three peaks, including pyridinic nitrogen (398.5 eV), pyrrolic nitrogen (400.2 eV) and quaternary nitrogen (401.3 eV).

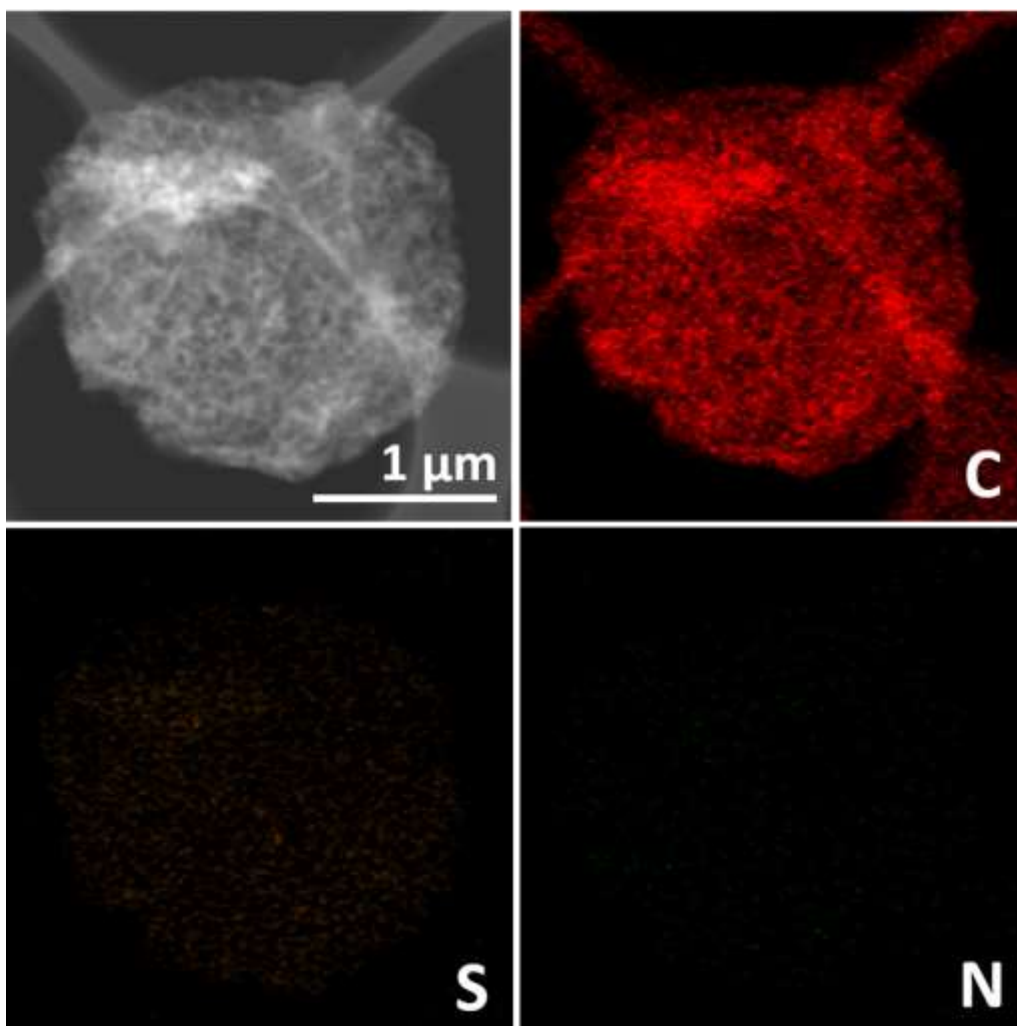


**Figure. S13.** TEM elemental mapping of 2D-HCA. It can be observed that the N and S elements were homogeneously distributed within the carbon framework.

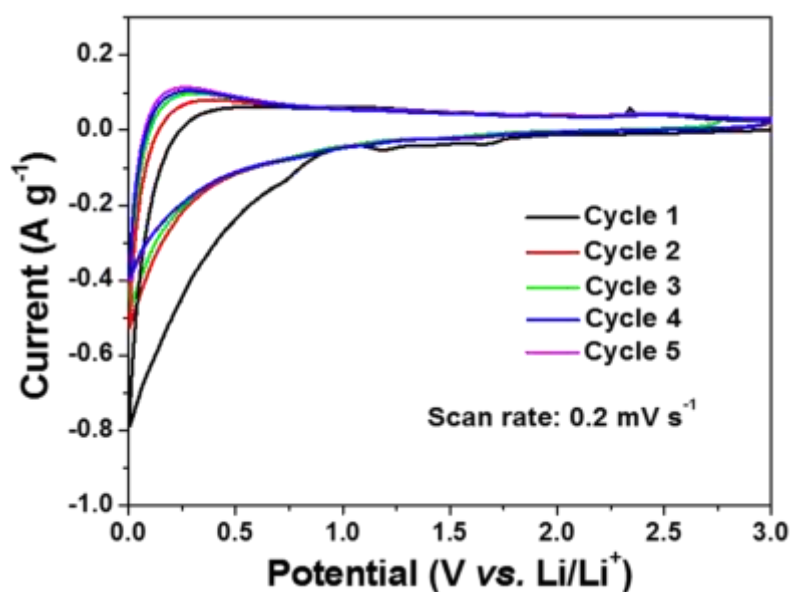


**Figure. S14.** CV curves of C-OII at a scan rate of  $0.2 \text{ mV s}^{-1}$ . The redox peaks near to 0 V can be attributed to  $\text{Li}^+$  ions insert into the graphite layers of C-OII. The oxidation peaks at  $\sim 0.2 \text{ V}$

related with the delithiation process of lithium ions from the graphite layers of C-OII. The current densities are much lower than that of 2D-HCA.

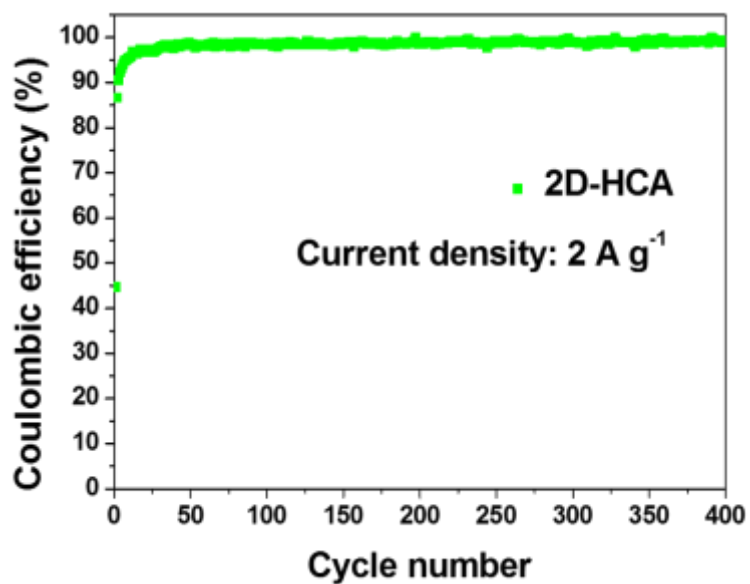


**Figure. S15.** Coulombic efficiency of 2D-HCA during long-term cyclability tests. The corresponding Coulombic efficiency at such high current density ( $2 \text{ A g}^{-1}$ ) reaches over 90 % in the initial 3 cycles and over 95 % after 8 cycles.

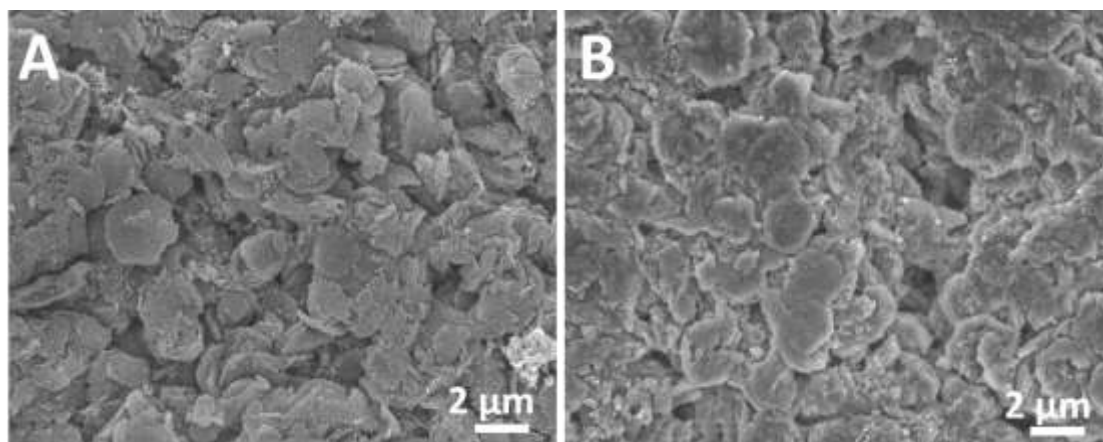


**Figure. S16.** SEM images of 2D-HCA electrodes before cycling (A) and after 20 cycles at a current density of  $200 \text{ mA g}^{-1}$  (B).

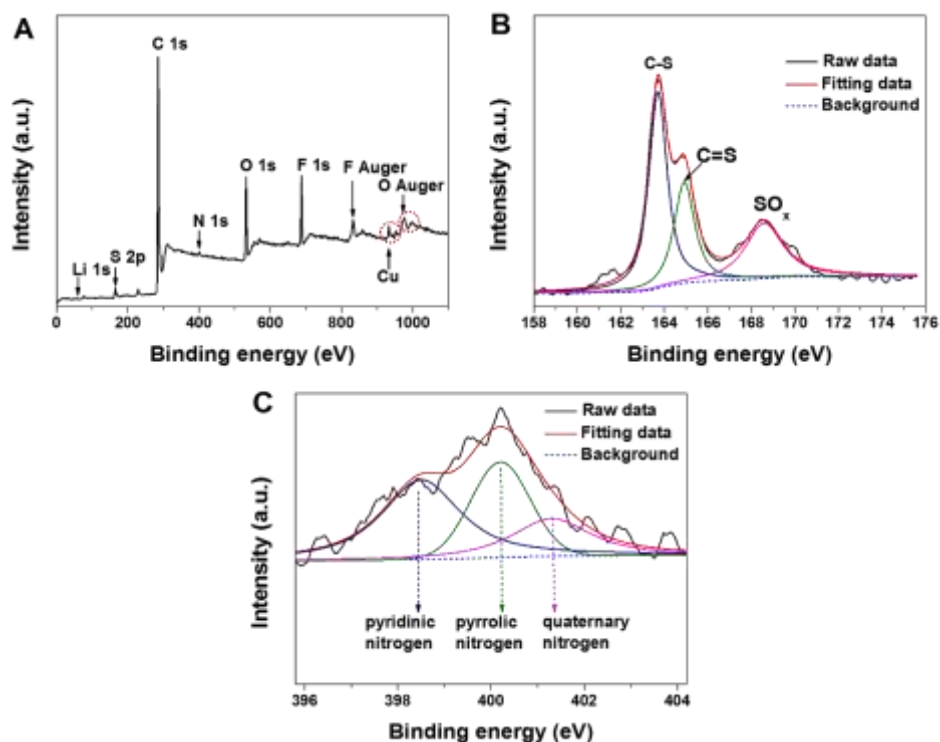


**Figure. S17.** XPS spectra of 2D-HCA electrode after 100 cycles (current density: 2 A g<sup>-1</sup>). (A) XPS survey spectrum of cycled 2D-HCA electrode; the corresponding high resolution XPS spectra of S 2p (B) and high resolution N 1s (C). The results revealed the N and S heteroatoms stably doped in the carbon framework. The N, S dual-doping nature can increase the electrochemical activity of the carbon framework. The F peak originated from PVDF and LiFP<sub>6</sub>, and the Li peak originated from LiFP<sub>6</sub> in electrolyte. The Cu peaks originated from the Cu current collector.